Journal of Molecular Liquids 296 (2019) 111916

Contents lists available at ScienceDirect

Journal of Molecular Liquids

journal homepage: www.elsevier.com/locate/molliq

Deep eutectic solvents based highly efficient extractive desulfurization of fuels – Eco-friendly approach

Patrycja Makoś, Grzegorz Boczkaj *

Gdansk University of Technology, Faculty of Chemistry, Department of Process Engineering and Chemical Technology, 80 – 233 Gdansk, G. Narutowicza St. 11/12, Poland

ARTICLE INFO

Article history:
Received 10 June 2019
Received in revised form 3 October 2019
Accepted 11 October 2019
Available online 16 October 2019

Keywords:
Deep eutectic solvents
Desulfurization
Diesel
Extraction
Fuel
Green chemistry

ABSTRACT

The developed process is based on alternative, green and cheap solvents for efficient desulfurization of fuels. Several deep eutectic solvents (DESs) were successfully synthesized and studied as extraction solvents for desulfurization of model fuel containing thiophene (T), benzothiophene (BT) and dibenzothiophene (DBT). The most important extraction parameters (i.e. kind of DES, DES: fuel volume ratio, hydrogen bond acceptor: hydrogen bond donor mole ratio, time of extraction and temperature) were optimized using central composite design model. Furthermore, the mutual solubility of DES and model fuel and influence of multistage extraction, reusability, regeneration of DES and content of aromatic groups in fuel are discussed followed by explanation of desulfurization mechanism, by means of density functional theory (DFT) as well as FT-IR analysis. The studies revealed high desulfurization effectiveness resulting in 91.5%, 95.4% and 99.2% removal of T, BT and DBT respectively in a single stage extraction. A three stage desulfurization provide >99.99% removal of T, BT and DBT. The research on the desulfurization mechanism revealed that π-π interaction is the main driving force for desulfurization process based on DES.

© 2019 The Authors. Published by Elsevier B.V. This is an open access article under the CC BY license (http://creativecommons.org/licenses/by/4.0/).

1. Introduction

The combustion of fuels containing sulfur compounds causes emission of toxic sulfur oxides (SO_x), which are a one of the main air pollutants [1]. Due to this fact, many countries have issued stringent standards to control the sulfur content of fuel oil (mainly below 10 mg/L) [2,3].

Nowadays, hydrodesulfurization (HDS) is the most popular commercial technology used for removal of sulfur from fuels. HDS can effectively remove sulfur compounds [4,5], however, HDS process is not effective for removing cyclic organic sulfides such as thiophene (T), benzothiophene (BT), dibenzothiophene (DBT) and its derivatives [6]. In addition, HDS requires large quantities of hydrogen, a high temperature and pressure of the process, and expensive Cobalt–Molybdenum catalysts. This makes HDS a very costly technology for removal of sulfur compounds from fuels. Therefore, many research groups work on the development of new technologies for deep desulfurization, such as adsorptive desulfurization [7], bio-desulfurization [8], oxidative desulfurization [9,10] or extraction [11–13]. Extractive desulfurization is one of the most popular techniques. It follows from its low cost, high sulfur removal efficiency and simplicity of operation. However, most extraction processes require the use of organic solvents, which are volatile, toxic and difficult for regeneration such as methanol, acetonitrile, sulfolane, and *N*-methyl-2-pyrolidone [13–16].

Since 2001, ionic liquids (ILs) have been widely considered green solvents because of their properties, such as non-volatility, non-flammability, high tunability, and high extraction efficiency [17]. However, ILs possess several major drawbacks: the high cost, difficulties in their synthesis, high viscosity and in some cases toxicity and related biodegradability issues [18–21].

A promising alternatives to ILs, which have similar unique physicochemical properties are deep eutectic solvents (DESs). DESs have a number of advantages such as simplicity and low cost of synthesis, easy biodegradation, non-toxicity and accessible raw material [22]. DESs are a liquids composed of two or more components, hydrogen bond acceptors (HBA) typically quarternary ammonium salts and hydrogen bond donors (HBD), whose melting points are lower than both of the individual components [23]. In recent years, DESs have been widely used in electrochemistry [24,25], catalysis [26], material preparation [27], nanotechnology [28], analytical chemistry [29–31], separation processes [32,33] etc. The non-toxic behavior in respect to human being results in several applications as a so-called therapeutic DESs [34]. In addition, several successful applications of DESs in desulfurization processes have been reported [35–38]. Among the existing literature, the DESs composed of quaternary ammonium salts as an HBA

* Corresponding author.
E-mail addresses: patrycja.makos@pg.edu.pl (P. Makoś), grzegorz.boczkaj@pg.edu.pl, grzegorz.boczkaj@gmail.com (G. Boczkaj).

https://doi.org/10.1016/j.molliq.2019.111916
0167-7322/© 2019 The Authors. Published by Elsevier B.V. This is an open access article under the CC BY license (http://creativecommons.org/licenses/by/4.0/).

and acids [35,39], glycols [36,40,41] and metal ions [42] as an HBD are the most used mixtures in desulfurization. The DESs composed of polyethylene glycol (PEG) allows removal of polycyclic organic sulfides from model fuel up to 85% in a single stage extraction [40,41]. Whereas the use of DES composed of tetrabutylammonium chloride (TBAC), PEG and a small addition of $FeCl_3$ (TBAC: PEG: $FeCl_3$ 4 : 1: 0.05 M ratio) allows the removal of DBT in 89.5% [36]. The desulfurization processes in which carboxylic acids were used as HBD, showed a lower efficiency which does not exceed 65% after one cycle of extraction [35,39]. Due to the numerous combinations of DES, still many mixtures that can provide higher desulfurization efficiency have not been studied. In addition, only a few papers have attempted to explain the mechanism of extractive desulfurization, which is necessary for farther industrial applications [42–47].

The paper describes for the first time an application of DESs composed of choline chloride (ChCl) acting as HBA and phenolic compounds as HBD, respectively for removal T, BT and DBT from model fuel. The extraction desulfurization was optimized in terms of selection of a DES, temperature, extraction time, HBA: HBD ratio and DES: model fuel ratio (V_{DES}:V_{Fuel}) using central composite design (CCD). The multistage extraction, reusability and regeneration of DES as well as influence of content of aromatic fraction in fuel on desulfurization yield were also investigated. For the better understand the mechanism of desulfurization, density functional theory (DFT) as well as FT-IR analysis was employed.

2. Experimental

2.1. Materials

The chemicals used for model liquid fuel preparation such as thiophene (purity ≥ 99%), benzothiophene (purity ≥ 95%) and dibenzothiophene (purity ≥ 98%), α-methylnaphthalene (purity ≥ 95%), n-hexadecane (purity 99%) were purchased from Sigma-Aldrich (USA), n-heptane (purity ≥ 99.9%) and diethyl ether (purity ≥ 99.9%) were procured from Merck (Germany). For DES synthesis choline chloride (ChCl), 4-chlorophenol (4CPh), 4-ethylphenol (4EtPh), phenol (Ph), 2-methylphenol (2MPh), 3-methylphenol (3MPh), 4-methylphenol (4MPh), and 2,6-dimethylphenol (2,6DMPh) were obtained from Sigma-Aldrich (USA). Compressed gases used for chromatographic analysis such as helium (purity N 5.5) (Linde Gas, Poland), hydrogen (purity N 5.5) generated by a PGXH2 500 Hydrogen Generator (PerkinElmer, USA) and air (purity N 5.0) generated by a DK50 compressor with a membrane dryer (Ekkom, Poland) and further purified by a GC3000 zero air generator (PerkinElmer, USA).

2.2. Apparatus

Gas chromatograph Autosystem XL equipped with an autosampler and a flame photometric detector (FPD) (PerkinElmer, USA), a DB-1 (60 m × 0.32 mm x 1.0 μm) capillary column (BGB, Switzerland), TurboChrom 6.1 software (PerkinElmer, USA) were used in the investigations. FT-IR spectra were recorded using a Bruker Tensor 27 spectrometer (Bruker, USA) with an ATR accessory and OPUS software (Bruker, USA). Dynamic viscosity was determined by means of BROOKFIELD LVDV-II + viscometer (Labo-Plus, Poland).

2.3. Procedures

2.3.1. Preparation of DES and model fuel

DESs were synthesized by mixing ChCl (HBA) and phenolic compounds (HBD) including Ph, 2MPh, 3MPh, 4MPh, 2,6DMPh, 4EtPh, and 4CPh in a mole ratio (HBA:HBD) of 1:2, 1:3, 1.4, 1:5 and 1:6 (Fig. S1). The mixture was stirred magnetically at 50 °C until a homogeneous liquid was obtained. The liquids were then left to cool spontaneously to room temperature.

The model fuel was prepared by dissolving T, BT and DBT in n-heptane. The initial concentration of T, BT and DBT was 500 mg/L.

2.3.2. Extractive desulfurization

The extraction was performed by mixing DES - ChCl: Ph (1: 4 M ratio) (10 mL) with the model fuel (4 mL) in a 40-mL beaker. The mixture was stirred for 40 min at 600 rpm at 40 °C. Then 1.5 mL of model fuels were transferred to 2-mL vials, followed by an addition of 10 μL of internal standard solutions (2-chlorothiophene) in n-heptane at a concentration of 300 mg/L. Then, the T, BT and DBT content of the model fuel was determined after each experiment using GC-FPD.

The efficiencies of the extraction were determined using equation (1):

$$E[\%] = \frac{C_{IN} - C_{Fin}}{C_{IN}} \cdot 100\% \quad (1)$$

where: C_{IN} – initial concentration of T, BT and DBT in the model fuel [mg/L], C_{Fin} – Final concentration of T, BT and DBT in the model fuel [mg/L].

The partition coefficients (K) were determined using equation (2):

$$K = \frac{C_{DES}}{C_{Fuel}} \quad (2)$$

where: C_{DES} – concentration of T, BT, DBT in the DES phase, C_{Fuel} – concentration of T, BT, DBT in the fuel phase after extraction.

2.3.3. Chromatographic analysis

The GC oven temperature program was as follows: 70 °C (1 min) – ramped at 30 °C/min to 320 °C (3 min). Injection port temperature was 300 °C. Injection mode: split 25:1.1 μL of the extract was injected into the GC system. FPD temperature was 320 °C, and detector gases flow rates were as follows: hydrogen 90 mL/min and air 75 mL/min.

2.3.4. FT-IR analysis

FT-IR spectra of pure DESs and DESs after extraction procedures were taken using attenuated total reflectance (ATR) with the following operating parameters: spectral range 4000–600 cm^{-1}, resolution: 4 cm^{-1}, number of sample scans: 256, number of background scans: 256, slit width: 0.5 cm.

2.3.5. Density and viscosity analysis

Dynamic viscosity was determined using 5 mL of DESs at RT (25 °C) and atmospheric pressure. Density was measured gravimetrically using 5 mL of DESs.

2.3.6. Mutual solubility of DES and model fuel and studies of fuel water washing

The mutual solubility of the model fuel (n-heptane) and DES as well as removal of DES traces from fuel by water washing was measured by gravimetric methods coupled with vacuum drying, according to a previously published method [3].

2.3.7. Theoretical study

The Orca 4.1.0 software package was used to optimize the molecular geometries and energy interaction between DES and sulfur compounds with density functional theory (DFT) using M06-2x/6–31 ++ G** level of theory. This level of theory is recommended to study ionic liquids as well as deep eutectic solvents [44–46]. All the configurations were tested to be local minima by frequency calculations. The interaction energy was therefore determined from (3):

$$E_{int} = E_{DES-S} - (E_{DES} + E_S) \quad (3)$$

where: $E_{complex}$-total energy of the complex formed by DES and sulfur compounds, E_{DES}- total energy of DES, E_S - total energy of sulfur

MOST WIEDZY Downloaded from mostwiedzy.pl

compounds. Lastly, counterpoise method has also been implemented to estimate the effects of the basis set superposition error (BSSE) on the interaction energy. The Multiwfn [48] and VMD software were used to perform Electrostatic potential (ESP) [49] and Reduced density gradient (RDG) analysis [50] to interpret the interaction nature in desulfurization process.

3. Results and discussion

3.1. Synthesis and physicochemical properties of DESs

Deep eutectic solvents composed of ChCl and phenols were synthesized according to the procedure described in our previous paper [31]. The most important physicochemical properties affecting extraction efficiencies such as density and viscosity were measured. The average molar masses of the deep eutectic solvents were also calculated. All properties of DESs are compiled in Table 1. The dynamic viscosity of the DESs for the same mole ratio can be approximately arranged in the following order: ChCl:4CPh > ChCl:2,6DMPh ≈ ChCl:4EtPh > ChCl:4MPh ≈ ChCl:3MPh ≈ ChCl:2MPh > ChCl:Ph. Densities of all DESs are higher than the model fuel ($\rho = 683.8$ kg/m^3) which is an advantage in the case of industrial applications. In all DESs, with the increase of HBD content in DES, viscosity and density values decreased.

3.2. Optimization of desulfurization conditions

3.2.1. Kind of HBD in DES

Kind of extraction solvent has a major effect on the desulfurization efficiency. Several deep eutectic solvents consisting of ChCl (HBA) and various HBDs, including Ph, 2MPh, 3MPh, 4MPh, 4EtPh, 2,6-DMPh and 4CPh in mole ratios (HBA:HBD) 1:2 were synthesized and their desulfurization capabilities were investigated. In the first experiment, the following pre-selected desulfurization conditions were used: extraction time 40 min, extraction temperature 20 °C and V_{DES}:V_{Fuel} 1 : 1. As indicated in Fig. 1, the desulfurization efficiencies followed the sequence for HBD of Ph > 2,6MPh >2MPh ≈ 3MPh ≈ 4MPh> 4EtPh > 4CPh. The obtained results indicate the relationship between polarity of DESs and extraction efficiency. It can be observed that along with a decrease in hydrophobicity of derivatives phenol in DESs the desulfurization efficiency increase.

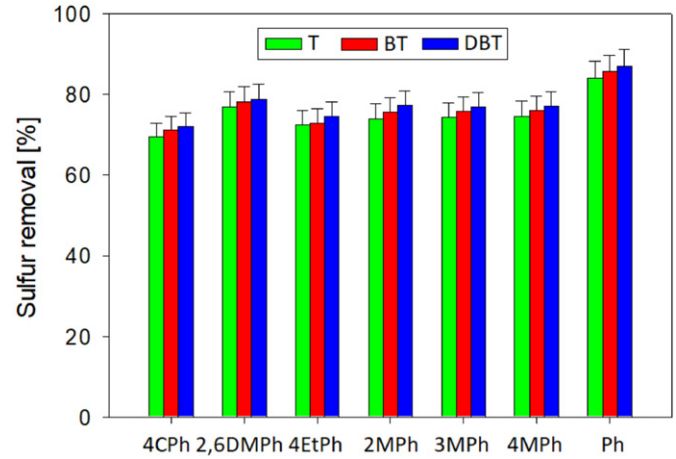

Fig. 1. The effect of kind of HBD in DESs on the desulfurization yield.

Table 1
Compilation of physicochemical properties of DESs.

DES	Mole ratio (HBA: HBD)	X_{HBA}	X_{HBD}	M_w [g/mol]	ρ [kg/m^3]	η [mPa·s]
ChCl: Ph	1 : 2	0.33	0.67	109.28	1098.9 ± 4.2	122.51 ± 5.27
	1 : 3	0.25	0.75	105.49	1094.1 ± 4.3	56.11 ± 2.13
	1 : 4	0.20	0.80	103.21	1091.5 ± 4.9	39.28 ± 1.41
	1 : 5	0.17	0.83	101.70	1089.1 ± 5.3	30.65 ± 1.20
	1 : 6	0.14	0.86	100.61	1088.1 ± 4.6	26.18 ± 0.79
ChCl: 2MPh	1 : 2	0.33	0.67	118.63	1071.2 ± 4.7	137.12 ± 5.61
	1 : 3	0.25	0.75	116.01	1065.1 ± 4.3	73.25 ± 3.22
	1 : 4	0.20	0.80	114.44	1062.1 ± 4.7	56.18 ± 2.58
	1 : 5	0.17	0.83	113.39	1060.1 ± 5.8	47.22 ± 2.31
	1 : 6	0.14	0.86	112.64	1059.0 ± 6.3	38.19 ± 1.82
ChCl: 3MPh	1 : 2	0.33	0.67	118.63	1071.8 ± 5.9	138.07 ± 6.63
	1 : 3	0.25	0.75	116.01	1065.9 ± 5.6	74.18 ± 3.41
	1 : 4	0.20	0.80	114.44	1062.8 ± 5.7	56.16 ± 2.59
	1 : 5	0.17	0.83	113.39	1061.1 ± 5.3	49.24 ± 2.22
	1 : 6	0.14	0.86	112.64	1059.1 ± 4.1	39.12 ± 1.56
ChCl: 4MPh	1 : 2	0.33	0.67	118.63	1072.1 ± 4.3	138.69 ± 3.45
	1 : 3	0.25	0.75	116.01	1066.6 ± 5.2	75.19 ± 2.82
	1 : 4	0.20	0.80	114.44	1063.4 ± 4.2	55.19 ± 1.99
	1 : 5	0.17	0.83	113.39	1061.1 ± 4.5	47.26 ± 1.44
	1 : 6	0.14	0.86	112.64	1059.9 ± 4.4	41.11 ± 1.23
ChCl: 4EtPh	1 : 2	0.33	0.67	127.98	1129.9 ± 5.1	143.25 ± 4.87
	1 : 3	0.25	0.75	126.53	1120.2 ± 5.2	84.18 ± 2.78
	1 : 4	0.20	0.80	125.65	1119.1 ± 5.5	62.12 ± 1.99
	1 : 5	0.17	0.83	125.07	1117.1 ± 5.8	53.08 ± 2.18
	1 : 6	0.14	0.86	124.65	1111.2 ± 5.4	49.12 ± 1.97
ChCl: 2,6DMPh	1 : 2	0.33	0.67	127.98	1130.9 ± 4.7	151.18 ± 6.96
	1 : 3	0.25	0.75	126.53	1127.9 ± 6.3	86.79 ± 3.04
	1 : 4	0.20	0.80	125.65	1125.8 ± 6.2	61.87 ± 1.92
	1 : 5	0.17	0.83	125.07	1123.9 ± 5.6	54.12 ± 2.06
	1 : 6	0.14	0.86	124.65	1122.4 ± 4.7	50.22 ± 1.62
ChCl: 4CPh	1 : 2	0.33	0.67	132.25	1203.1 ± 6.1	180.25 ± 5.59
	1 : 3	0.25	0.75	131.33	1199.8 ± 6.2	108.18 ± 3.25
	1 : 4	0.20	0.80	130.77	1198.2 ± 5.9	77.89 ± 2.96
	1 : 5	0.17	0.83	130.40	1197.6 ± 5.0	66.12 ± 2.52
	1 : 6	0.14	0.86	130.14	1196.5 ± 5.2	61.06 ± 2.02

M_W– molar mass, calculated from $M_W = x_{HBA} \cdot M_{HBA} + x_{HBD} \cdot M_{HBD}$, where: x_{HBA}-mole fraction of HBA, M_{HBA}– molar mass of HBA [g/mol], x_{DHB}– mole fraction of HBD, M_{HBD}–molar mass of HBD [g/mol], η – dynamic viscosity, ρ – density [kg/m^3].

MOST WIEDZY Downloaded from mostwiedzy.pl

Table 2
Experimental ranges and levels of two variables in CCD.

Variables	Coded Name	Ranges and levels (star points = $(2^k)^{1/4} = 2$) [a]				
		-α	−1	0	+1	+α
V_{DES}:V_{Fuel}	X_1	0.5 : 1	1 : 1	1.5 : 1	2 : 1	2.5 : 1
ChCl: Ph mole ratio	X_2	1 : 2	1 : 3	1 : 4	1 : 5	1 : 6
Time of desulfurization [min]	X_3	10	20	30	40	50
Temperature [°C]	X_4	20	30	40	50	60

[a] k – number of variables = 3.

3.2.2. Central composite design

In the next step, four parameters were used to plan a subsequent higher order 2^2 design by means of Central Composite Design. CCD consists of selection of five experimental points: edge points (+1 and −1) corresponding to the upper and lower limits of the investigated factor, star points (-α and +α) and zero levels. The variables evaluated were V_{DES}:V_{Fuel} from 0.5:1 to 2.5:1, ChCl: Ph mole ratio (1:2–1:6), time of extraction (10–50 min) and temperature (20–60 °C). Table 2 demonstrated extended values for all parameters in five levels and the design matrix and responses for the percentage of removal of sulfur compounds from model fuel are given in Table S1.

The data obtained were evaluated by analysis of variance (ANOVA) and regression in order to create an appropriate model and select statistically important and effective factors. In ANOVA, the statistical F- and p-values were adopted as criteria at a 95% confidence level. The p-value reveals the significance of each coefficient and explains the interaction pattern of independent variables. The parameters with p-value less than 0.05 were considered as statistically significant and influential on the statistic model. According to the analysis of variance, the p-value of the models was found to be statistically significant due to the p-value <0.0001 for T, BT and DBT and F-values equal to 72.46, 73.52 and 27.79 for T, BT and DBT respectively. The p-values (>0.38) of lack of fit relative to the pure error were considered insignificant.

Tables S2–S4 present the ANOVA results for response surface quadratic model.

The response equations obtained for experimental results can be expressed as follow:

$$Y_{(T)} = 86.54 + 5.02\,X_1 + 1.66\,X_2 + 4.91\,X_3 - 2.81\,X_1^2 - 1.22\,X_2^2 - 2.96\,X_3^2 - 6.92\,X_4^2 - 1.12X_{1*}X_3 \quad (4)$$

$$Y_{(BT)} = 93.64 + 9.76\,X_1 + 3.62\,X_2 + 10.05\,X_3 + 1.69\,X_4 - 11.74\,X_1^2 - 5.42\,X_2^2 - 11.82\,X_3^2 - 28.23\,X_4^2 - 3.74\,X_{1*}X_3 - 3.97\,X_{3*}X_4 \quad (5)$$

$$Y_{(DBT)} = 96.56 + 4.60\,X_1 + 4.48\,X_2 + 3.64\,X_3 - 2.07\,X_1^2 - 3.33\,X_2^2 - 3.22\,X_3^2 - 16.07\,X_4^2 + 3.25\,X_{2*}X_3 \quad (6)$$

where Y is the percentage removal of T, BT and DBT; X_1, X_2, X_3, X_4 are the independent variables. These equations explain the influence of the tested parameters on the desulfurization efficiency of T, BT and DBT. The developed models presented a high determination coefficient (R^2 = 98.54, 98.56 and 96.01% for T, BT and DBT respectively) along with the values of predicted (R^2_{pred} = 93.41, 93.39 and 85.12%) and adjusted determination coefficient (R^2_{adj} = 97.18, 97.22 and 92.29%). The obtained results indicate a good fit of the model to the experimental values and the possibility of prediction of responses for new data.

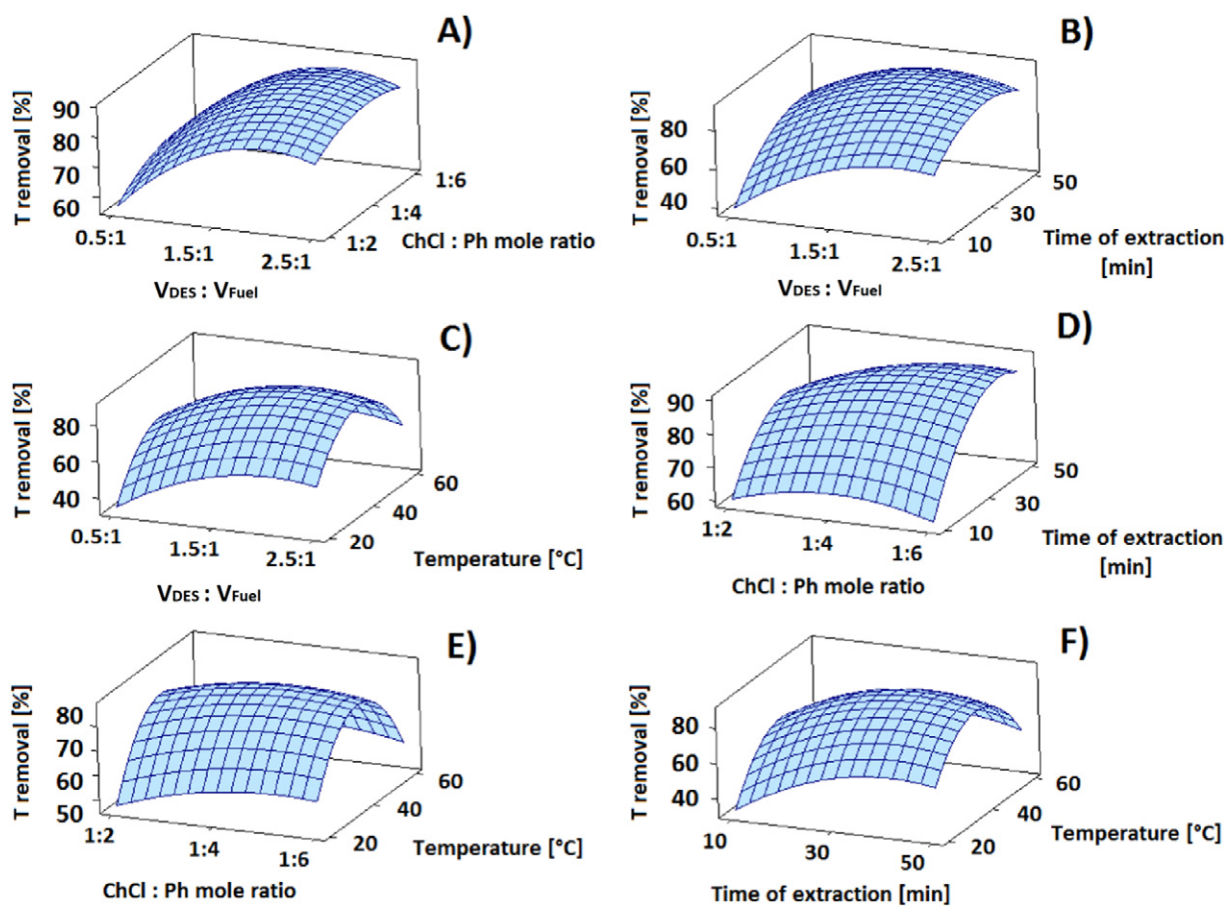

Fig. 2. Response surface plots for T surface area dependence on: A) V_{DES}:V_{Fuel} and ChCl: Ph mole ratio, B) V_{DES}:V_{Fuel} and time of extraction, C) V_{DES}:V_{Fuel} and temperature, D) ChCl: Ph mole ratio and time of extraction, E) ChCl: Ph mole ratio and temperature, F) time of extraction and temperature.

MOST WIEDZY Downloaded from mostwiedzy.pl

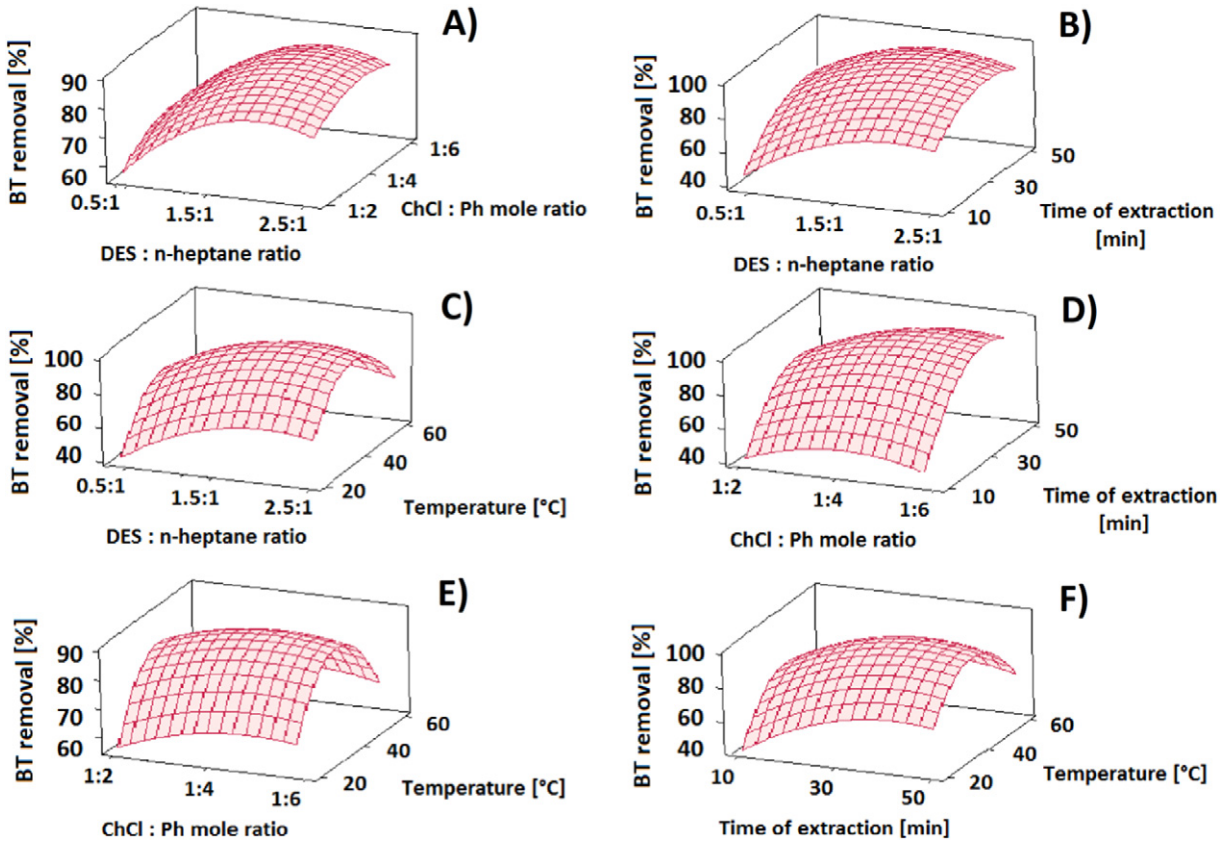

Fig. 3. Response surface plots for BT surface area dependence on: A) V_{DES}:V_{Fuel} and ChCl: Ph mole ratio, B) V_{DES}:V_{Fuel} and time of extraction, C) V_{DES}:V_{Fuel} and temperature, D) ChCl: Ph mole ratio and time of extraction, E) ChCl: Ph mole ratio and temperature, F) time of extraction and temperature.

3.2.3. Interaction effect

In order to note the effect of independent variable interactions, surface plots were illustrated that revealed several trends in response to the studied variables in relation to T, BT and DBT removal (Figs. 2–4). The results indicate that the most pronounced effect on the desulfurization of T, BT and DBT yield have V_{DES}:V_{Fuel}, ChCl:Ph molar ratio as well as time of extraction (p-value < 0.012).

From the economical aspect, the volume of DES should be as low as possible while achieving high extraction efficiency. On the other hand, the experimental results revealed that along with the increase V_{DES}:V_{Fuel} the desulfurization efficiency increases (Figs. 2–4 A,B,C).This is related to the fact that increase of V_{DES}:V_{Fuel} provide to increase ratio of the active hydrogen ratio to model fuel, which plays a dominant role in the desulfurization process based on DES [39].

ChCl:Ph molar ratio is also an important factor for desulfurization of T, BT and DBT. The results indicated that the increase of HBD content in DES leads to increase in extraction efficiency. The maximum of desulfurization yield was observed for 1:4 ChCl:Ph molar ratio. Further increase in phenol content in DES did not improved the desulfurization efficiency (Figs. 2–4 A,D,E). This could be explained by a significant decrease in viscosity with increasing HBA:HBD molar ratio from 1:2 to 1:4. Further increase in the phenol content in DES only slightly lowers the viscosity values.

The experimental results revealed that along with the increase of extraction time, the desulfurization efficiency increases, probably due to the increasing solubility of sulfur compounds in DES during mixing, which increased the mass transfer of T, BT and DBT from fuel to DES phase. In all cases, the maximum extraction efficiency was achieved after 40 min (Figs. 2–4 B,D,F). Further extension of time did not improved the extraction yield due to the fact that the extraction process have reached equilibrium.

From the economical point of view, lower temperature is beneficial because of a lower energy consumption. In Figs. 2–4 C,E,F, it can be seen that with the increase of extraction temperature from 20 to 40 °C, the extraction efficiencies increases. Further increasing of temperature from 40 to 60 °C results in decrease of desulfurization yield. Too high temperature is not favorable due to the fact that the interactions between DES and sulfur compounds are based on an exothermic reaction and are described by Van't Hoff law, which describes that for an exothermic reaction heat is released, making the net enthalpy change negative, which has a direct impact of the partition coefficient value between DES and fuel [32,39,51]. On the other hand, too low temperature results in insufficient extraction efficiency.

Among the interaction of parameters, statistically the highest impact on the desulfurization efficiency has the ratio of V_{DES}:V_{Fuel} and time of desulfurization (p value < 0.042) for T and BT as well as temperature and time of desulfurization (p value = 0.031) for BT and ChCl:Ph mole ratio and time of desulfurization (p value = 0.024) for DBT.

The desulfurization efficiency in all experiments followed the trend of DBT > BT > T. This is related to the increase of electron density of the sulfur atom in the order of TH < BT < DBT [40,42,52].

Overall, summarizing the results of optimization yields, the following optimum desulfurization conditions: ChCl: Ph (1 : 4 M ratio); V_{DES}:V_{Fuel} 2.5 : 1; extraction time 40 min and temperature 40 °C.

3.2.4. Multistage extraction

The desulfurization with multiple cycles was also investigated to find the number of needed extraction stages for achieving ultra-low sulfur content fuels. In the investigations, at the end of each cycle of extraction, the phase of raffinate was transferred to a clean beaker then fresh DES was added to the next extraction cycle. All extraction stages were carried out under the same conditions. For DES as extractant, the

MOST WIEDZY Downloaded from mostwiedzy.pl

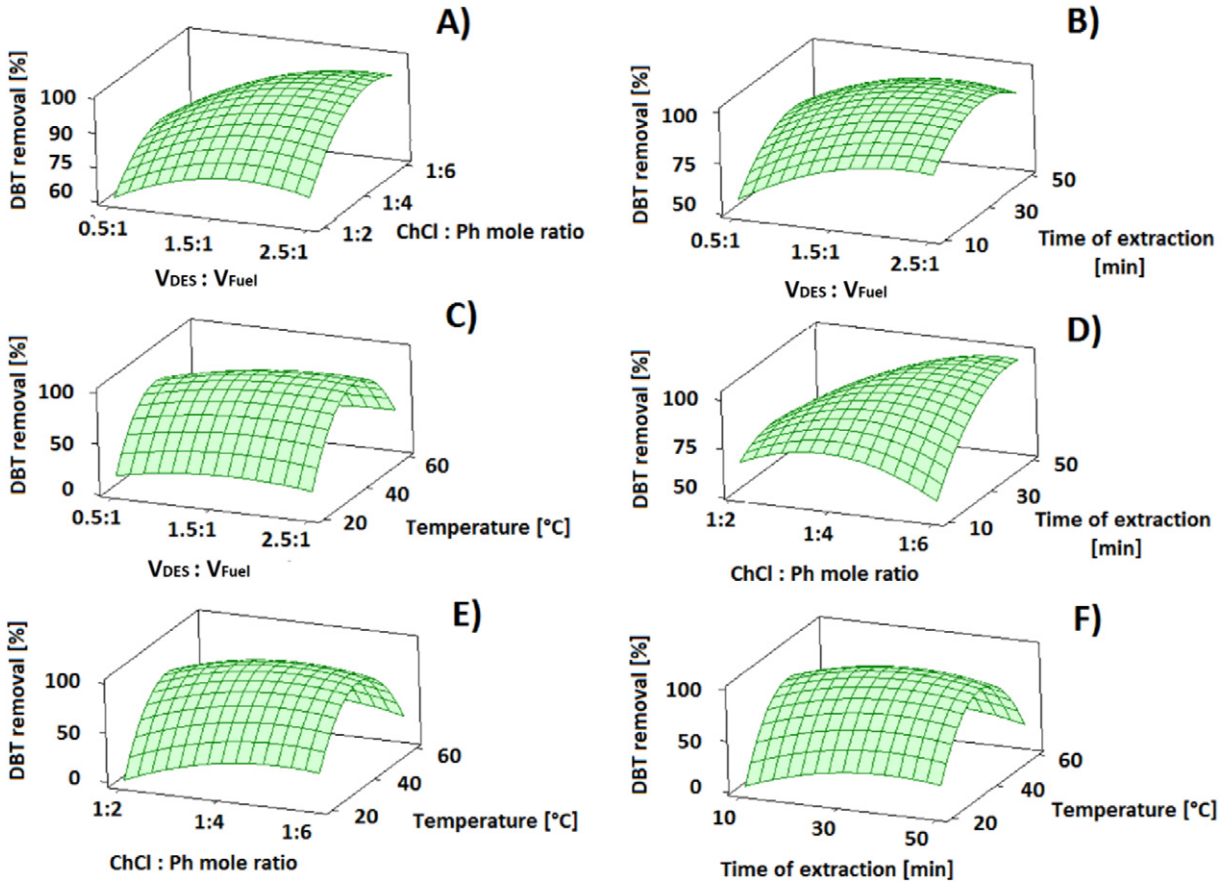

Fig. 4. Response surface plots for DBT surface area dependence on: A) V_{DES}: V_{Fuel} and ChCl: Ph mole ratio, B) V_{DES}: V_{Fuel} and time of extraction, C) V_{DES}:V_{Fuel} and temperature, D) ChCl: Ph mole ratio and time of extraction, E) ChCl: Ph mole ratio and temperature, F) time of extraction and temperature.

desulfurization efficiency was 91.5% (42.9 mg/L), 95.4% (23.1 mg/L) and 99.2% (3.9 mg/L) for T, BT and DBT respectively at one step of extraction. The partition coefficients were as follow 10.7, 20.65 and 127.21 for T, BT and DBT. The concentrations of T, BT and DBT in model fuel after two steps were 3.73, 0.55 and 0.1 mg/L respectively. After three steps, the removal of T, BT and DBT reaches up to 99.99% (Fig. S2).

3.2.5. Reusability of DES

From an industrial point of view, solvent consumption should be minimized. According to this aspect, the capacity of DES without regeneration was also examined. The results indicate gradual decrease in extraction efficiency after the next extraction stage (Fig. S3). After five cycles of repeated extraction without regeneration, the desulfurization efficiency was lower than 52%, 55% and 61% for T, BT and DBT respectively, due to the saturation of DES with sulfur compounds.

3.2.6. Regeneration of DES

From the economic aspect, the recycling and reuse of extraction solvents is after the desulfurization process is highly desirable. Fortunately, DESs could be successfully recycled with traditional solvents [35,53]. In the investigation, DES was recycled by washing with diethyl ether (DES: diethyl ether 1:1), because of its ease of regeneration and purification [54,55]. The saturated DES was stirred for 1 h and then diethyl ether was removed from beaker. As shown in Fig. S4, DES can be recycled 15 times without noticeable decrease in extraction efficiency. On average, after regeneration, DES contained 47.5, 27.9 and 10.3 mg/L of T, BT and DBT, respectively.

3.2.7. Extractive desulfurization of different model fuels

Seven kinds of model fuels with different content from 0 to 60% of aromatic compounds (α-methylnaphthalene in n-hexadecane) were prepared to investigate the extractive performance of the DES. Compounds selected for the preparation of model fuel mixtures correspond to the components used in the reference fuels for determination of the cetane number [56]. The results indicate only a slight decrease in extraction efficiency with increasing of α-methylnaphthalene concentration in fuel (Fig. S5). Thus, extraction with DES as extractants may be a promising technology for desulfurization of different fuel fractions. The effect of fuel composition will not affect the purification effectiveness.

3.2.8. Mutual solubility of DES and model fuel and final fuel treatment by water washing

Mutual solubility of DES and fuel is an important parameter due to the fact that the solubility of DES in fuel would cause its contamination as well as loss of DES during the extraction process. Same aspect relates to the loss of fuel in case of its solubility in DES. Therefore, the extraction system should have minimum cross-solubility. The research indicates after extraction process DES contained 0.52% of n-heptane while n-heptane contained 0.37% of DES. These values suggest that model fuel and DES have low mutual solubility. The results are comparable with other DES [3,35,40,42]. However, due to the hydrophilic character of DES used in these studies, it should be possible to remove it from fuel by washing with clean water. This concept is widely used in fuel processing – a MEROX process is a one of most widely known examples. Our studies revealed that application of

MOST WIEDZY Downloaded from mostwiedzy.pl

clean water is effective for quantitative removal of the amounts of DES remaining in the fuel after extraction process.

3.3. Mechanism of desulfurization

The results of theoretical studies indicated that non-bonded interaction exist between Ch^+ and $Cl^-$and such as O–H···Cl (2.35 Å) and between Cl^- and three Ph molecules such as Cl···H–O (2.27 Å), Cl···H–O (2.30 Å) and Cl···H–O (2.27 Å) which can be identified as a strong hydrogen bonds due to short distance between atoms (below 2.5 Å) [57]. However, there is no hydrogen bonds between Cl- and the fourth Ph molecule. On the basis of distance, it can be concluded that there is weak electrostatic bond between Cl···H–O (3.77 Å) (Fig. 5). In the desulfurization process, the S atom can act as an acceptor in O–H···S and C–H···S as well as a donor in S–H···π interaction [58–63]. However, the optimized configurations of DES-T, DES-BT, and DES-DBT indicated, that between DES and sulfur compounds there are no hydrogen bonds. This is probably due to steric hindrance. Therefore, other interactions must play a key role on the desulfurization effect. The length of hydrogen bonds in DES did not change significantly after the introduction of T, BT, and DBT, which indicates that the structure of DES is stable during the desulfurization process (Fig. 5).

Electrostatic potential analysis (ESP) is very important for non-covalent systems in extraction or separation systems. For non-covalent interaction hydrogen bonding, van der Waals interactions and other interactions may coexist, and all of these may play important roles in weak interactions for non-covalent systems. The ESP analysis was adopted to qualitatively understand the configurations of DES as well as DES-T, DES-BT and DES-DBT systems. The ESP are mapped onto their electron densities in Fig. 6. The results demonstrated that the negative electrostatic potential region is around Cl and O atoms in HBA, while the positive electrostatic potential region is around H and N atoms. The electropositive areas of HBDs which are located around the H atom in the OH groups are attracted to the electronegative areas of HBDs during the formation of the DES. The stable configuration of DES is in accordance with monomer models of ChCl and Ph as well as in accordance with ESP analysis. The ESP analysis results of T, BT and DBT indicated that the electropositive area is around sulfur compounds while the negative area is at the inner cycle of these molecules. When T, BT or DBT molecules interacts with DES, the electropositive region located inside the benzene ring in HBD is attracted to the electronegative area in inside the rings of sulfur compounds, forming π-π interactions. Similar results were also observed in previous studies [42].

Reduced density gradient analysis (RDG) is a useful tool reveals the underlying chemistry that compliments the covalent structure and provides a rich representation of hydrogen bonds, van der Waals interactions, and steric repulsion among others in molecular complexes *i.e.* ILs or DES [42]. The RDG analysis was used to visualized weak non-

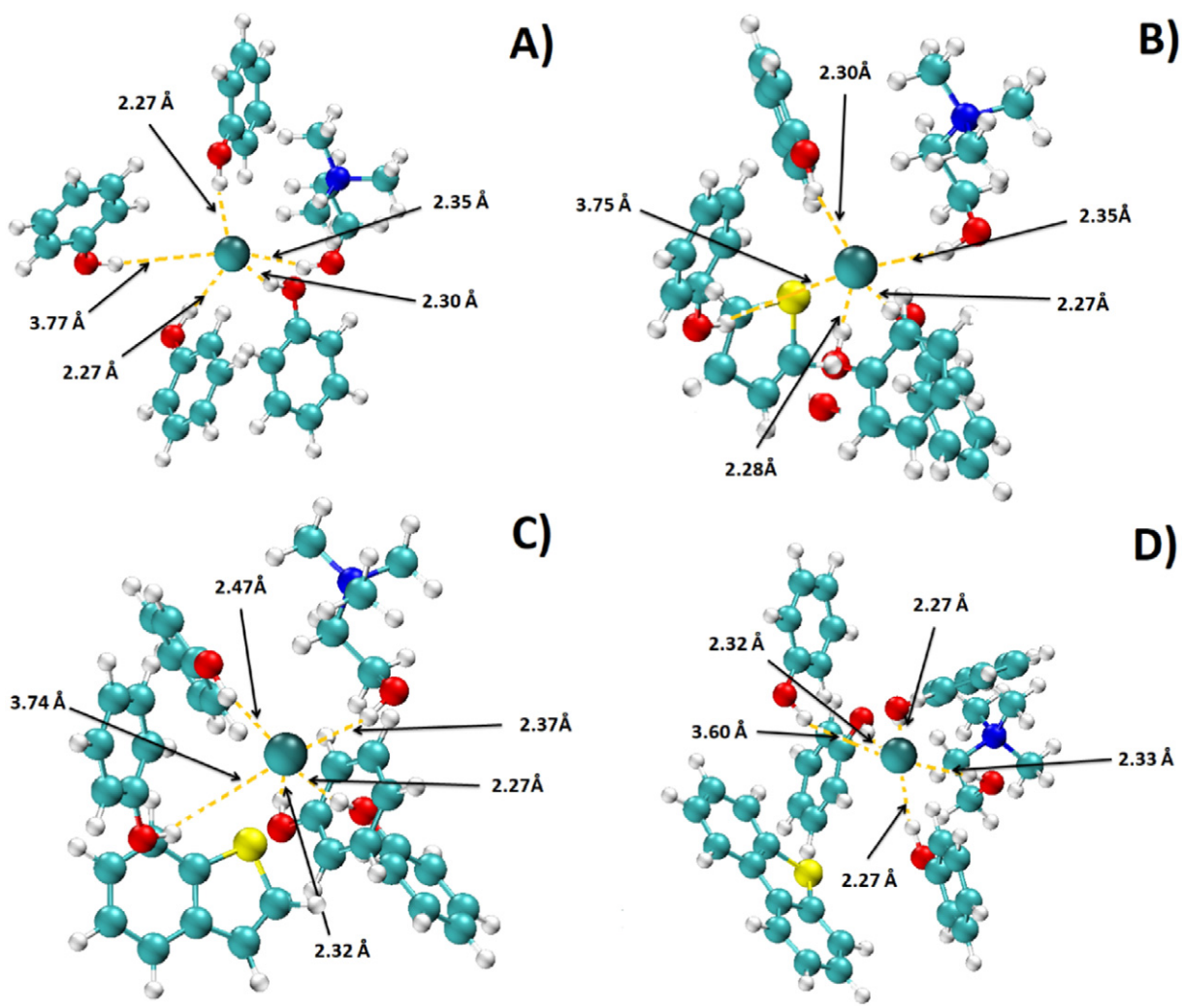

Fig. 5. Optimized configurations of A) DES, B) DES-T, C) DES-BT, D) DES-DBT.

MOST WIEDZY Downloaded from mostwiedzy.pl

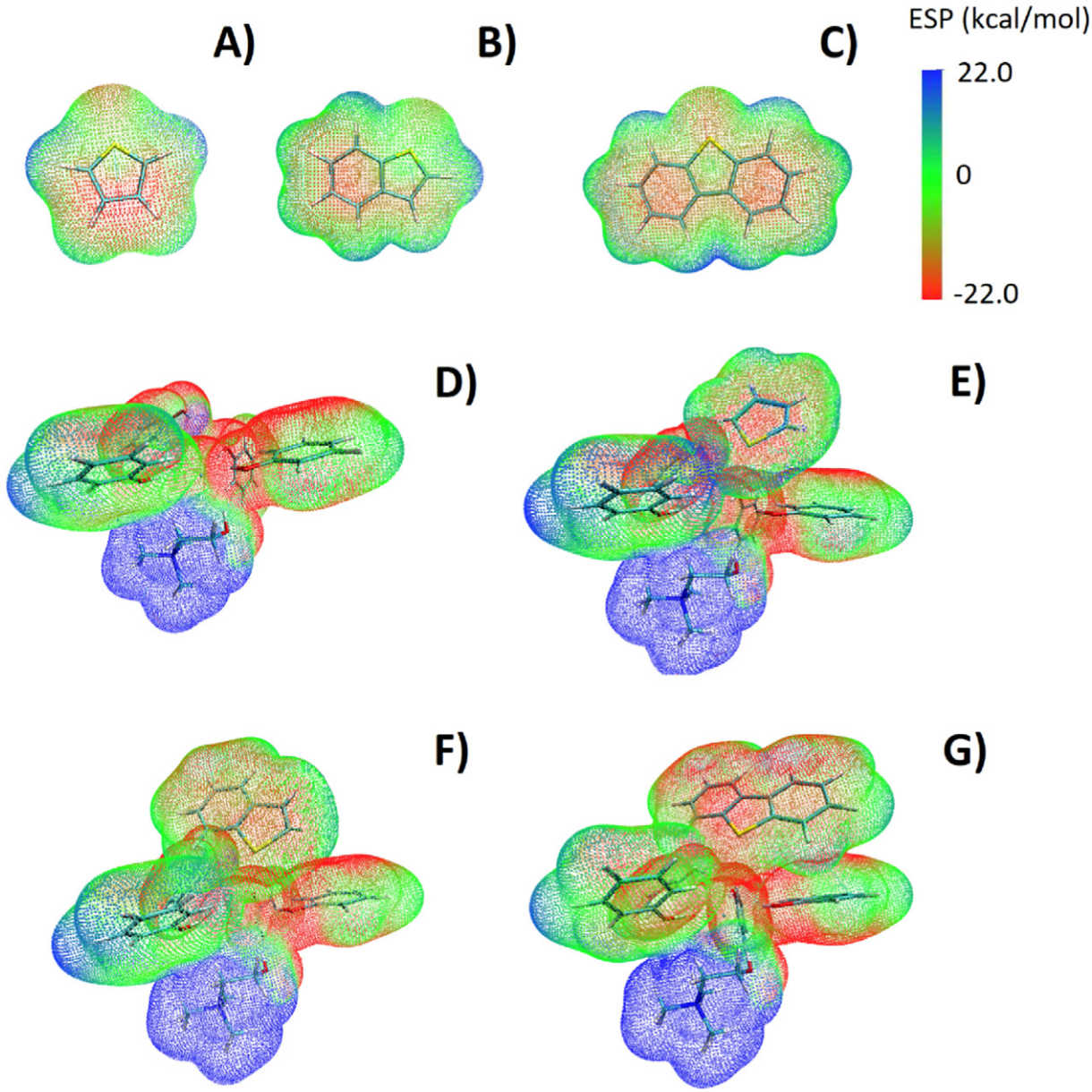

Fig. 6. ESP mapped on electron total density with an isovalue 0.001 for A) T, B), BT), C), DBT, D) DES, E) DES-T, F) DES-BT, G) DES-DBT. The corresponding electrostatic potential surfaces are depicted, with blue and red colors indicating the regions with positive and negative charges, respectively.

covalent interactions, by plotting the RDG versus the electron density multiplied by sign of the second Hessian eigenvalue [50]. Figs. S5–S7 and Fig. 7 and indicate that, hydrogen bonds, as well as van der Waals interactions and the steric effect, occur in the DES molecule and DES-T, DES-BT and DES-DBT complexes. Fig. S5 demonstrated that the hydrogen bonds are found between the Cl atom in HBA and the three H atoms in HBD (blue circle), in turn, the fourth phenol interacts with the HBA by the van der Waals interaction (green surface). The coexistence of both type of interactions in the monomer structure of the DES, which are responsible for the decrease in melting points and formation of DES. The result is consistent with previous considerations. The main interactions affecting the desulfurization process are van der Waals surfaces, between DES and sulfur compounds. The surfaces of these interactions increase follow the order of T < BT < DBT (Figs. S7–S8 and Fig. 7).

The value of interaction energy in the gas phase between DES and sulfur compounds is usually negative. A more negative value of E_{int} stands for stronger interaction between DES and T, BT and DBT. The calculated E_{int} values were – 4.9, −6.3, −8.7 kcaL/mol for T, BT and DBT respectively. The interactions energy followed a similar trend to that of experimental desulfurization efficiency (T < BT < DBT).

In order to verify the theoretical considerations of the desulfurization mechanism, FT-IR analysis were prepared. The spectrum of pure DES was compared with DES containing T, BT and DBT in different molar ratios (DES: S-compound 1 : 0.05 and 1 : 0.15). Figs. S9–S11 indicates the peak corresponding to stretching vibrations of the O–H (3270.5 cm^{-1}) stays in the same position after addition T, BT or DBT to DES. The peak shifts towards lower values in this region indicate the formation of hydrogen bonds in the studied complex [31,64]. However, FT-IR spectra after extraction indicate appearance of new peak at the 1420.8 and 708 cm^{-1} energy bands, which were absent in pure DES spectrum. This indicates the occurrence of the π–π interactions between unsaturated bonds of T, BT and DBT and OH–Cl association in ChCl:Ph. Similar results were also observed in previous research [42,65].

MOST WIEDZY Downloaded from mostwiedzy.pl

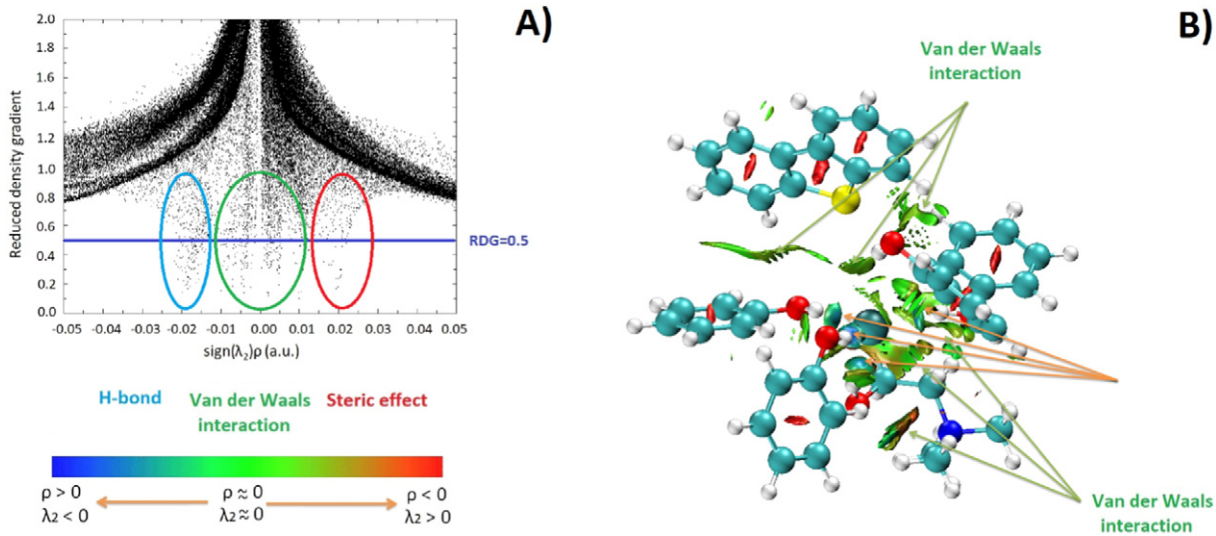

Fig. 7. A) Plots of electron density and its reduced density gradient for DES-DBT, B) Gradient isosurfaces (s = 0.5 a.u.) for DES-DBT (green surfaces indicate van der Waals interaction, blue – H-bond).

Table 3
Comparison of the developed procedure of desulfurization with other extractive desulfurization procedures based on DES.

Deep eutectic solvent (HBA: HBD)	Price of DES[a)]	V_{DES}:V_{Fuel}	Extractiontime [min]	Temp. [°C]	S-compound	S-content [mg/L]	Desulfurizationyield [%][b)]	Ref.
TBAB: FA (1 : 1)	170 $	1 : 1	30	30	T	500	55.8	[35]
					DBT	500	60	
TBAC: PEG:$FeCl_3$ (4 : 1: 0.05)	1500 $	1 : 1	15	25	DBT	1600	89.5	[36]
ChCl: Pr (1 : 3)	45 $	3 : 1	10	37	DBT	1600	65	[39]
TBAC:PEG (1 : 2)	600 $	1:1	15	RT	T	500	68	[40]
					DBT	500	85	
TBAB: PEG (1 : 2)	120 $	1:1	30	RT	T	500	62.2	[41]
					DBT	500	82.4	
TBPB: $FeCl_3$(1 : 2)	250 $	1 : 1	163	30	T	500	44	[42]
					DBT	500	64	
ChCl:Ph (1:4)	20 $	2.5 : 1	40	40	T	500	91.5	This work
					BT	500	95.4	
					DBT	500	99.2	

[a] Price per 1 kg of DES.
[b] Desulfurization yield in one stage of extraction.

Therefore, it can be concluded that van der Waals interactions are the main driving force for desulfurization process.

3.4. Comparison of the developed DES for desulfurization with literature procedures

A comparison of the developed desulfurization method based on ChCl:Ph (1:4) with other procedures for removal of sulfur compounds from model fuel revealed that the proposed procedure has higher desulfurization yield in single stage extraction. One of the most important parameters in industrial desulfurization applications is a price of organic solvents. DESs are considered as cheap solvents, but their price can vary significantly depending on the compounds used to synthesize them. DESs price can vary from 20 $ to 1500 $ per 1 kg. The price is mainly influenced by the type of HBA. Among available HBA based on quaternary ammonium salts, the cheapest is ChCl, which makes the price of ChCl:Ph competitive to the other DESs.

A comparison of the available extraction desulfurization procedures based on DES is provided in Table 3.

FA - formic acid, Pr - Propionic acid, TBAB - tetrabutylammonium bromide, TBAC - tetrabutylammonium chloride, TBPB - tetrabutylphosphonium bromide.

4. Conclusions

The environmentally friendly deep eutectic solvent ChCl:Ph was successfully applied for desulfurization of model liquid fuel. Effect of some extraction parameters including kind of DES, V_{DES}:V_{Fuel}, HBA:HBD mole ratio, time of extraction and temperature were also investigated. It was found that the optimum parameters of desulfurization were extraction solvent ChCl:Ph (1 : 4 M ratio), V_{DES}:V_{Fuel} 2.5 : 1; extraction time 40 min and temperature 40 °C. In optimal conditions, T, BT and DBT was removal in 91.5, 95.4 and 99.2% respectively via a one-step process. After three cycles, extractive desulfurization yield achieved as high as 99.99%. Compared with DESs described in the literature, the sulfur removal ability of ChCl:Ph is improved and its price is lower.

From the economic and industrial point of view, it's important to recycling of the solvent stream without regeneration. The results indicate that after five cycles of recycling, the

MOST WIEDZY Downloaded from mostwiedzy.pl

efficiency of desulfurization is reduced to around 50–60%, and DES needs to be regenerated. Fortunately, DES can successfully be regenerated by means of back-extraction with cheap diethyl ether and even after fifteen recycled times decrease in activity is not observed.

The research on the desulfurization mechanism revealed that π-π interaction is the main driving force for desulfurization process based on DES.

The ChCl:Ph (1:4) can be regarded as promising cheap non-toxic solvents for highly efficient desulfurization of liquid fuels and have potential for "green" industrial applications.

Conflict of interest statement

The authors have declared no conflict of interest.

Acknowledgements

The authors gratefully acknowledge the financial support from the National Science Centre, Warsaw, Poland – decision no. UMO-2018/30/E/ST8/00642.

Appendix A. Supplementary data

Supplementary data to this article can be found online at https://doi.org/10.1016/j.molliq.2019.111916.

References

[1] International Energy Agency, Energy and air pollution, world energy outlook special report, https://www.iea.org/publications/freepublications/publication/WorldEnergyOutlookSpecialReport2016EnergyandAirPollution.pdf, Accessed date: 17 September 2018.
[2] S.A. Dharaskar, K.L. Wasewar, M.N. Varma, D.Z. Shende, K.K. Tadi, C.K. Yoo, Synthesis, characterization, and application of novel trihexyltetradecylphosphoniumbis (2,4,4-trimethylpentyl) phosphinate for extractive desulfurization of liquid fuel, Fuel Process. Technol. 123 (2014) 1–10, https://doi.org/10.1016/j.fuproc.2014.02.001.
[3] C.F. Mao, R.X. Zhao, X.P. Li, X.H. Gao, Trifluoromethanesulfonic acid-based DESs as extractants and catalysts for removal of DBT from model oil, RSC Adv. 7 (2017) 12805–12811, https://doi.org/10.1039/C6RA28448E.
[4] A. Fihri, R. Mahfouz, A. Shahrani, I. Taie, G. Alabedi, Pervaporative desulfurization of gasoline: a review, Chem. Eng. Process 107 (2016) 94–105, https://doi.org/10.1515/aep-2015-0013.
[5] V.C. Srivastava, An evaluation of desulfurization technologies for sulfur removal from liquid fuels, RSC Adv. 2 (2012) 759–783, https://doi.org/10.1039/C1RA00309G.
[6] R. Javadli, A. Klerk, Desulfurization of heavy oil, Appl. Petrochem. Res. 1 (2012) 3–19, https://doi.org/10.1007/s13203-012-0006-6.
[7] J.M. Kwon, J.H. Moon, Y.S. Bae, D.G. Lee, H.C. Sohn, C.H. Lee, Adsorptive desulfurization and denitrogenation of refinery fuels using mesoporous silica adsorbents, Chem. Sus. Chem. 1 (2008) 307–309, https://doi.org/10.1002/cssc.200700011.
[8] S. Bhatia, D.K. Sharma, Biodesulfurization of dibenzothiophene, its alkylated derivatives and crude oil by a newly isolated strain PantoeaagglomeransD23W3, Biochem. Eng. J. 50 (2010) 104–109, https://doi.org/10.1016/j.bej.2010.04.001.
[9] J. Wang, L. Zhang, Y. Sun, B. Jiang, Y. Chen, X. Gao, H. Yang, Deep catalytic oxidative desulfurization of fuels by novel Lewis acidic ionic liquids, Fuel Process. Technol. 177 (2018) 81–88, https://doi.org/10.1016/j.fuproc.2018.04.013.
[10] Y. Gao, Z. Lv, R. Gao, G. Zhang, Y. Zheng, J. Zhao, Oxidative desulfurization process of model fuel under molecular oxygen by polyoxometalate loaded in hybrid material CNTs@MOF-199 as catalyst, J. Hazard Mater. 359 (2018) 258–265, https://doi.org/10.1016/j.jhazmat.2018.07.008.
[11] E. Kianpour, S. Azizian, M. Yarie, M.A. Zolfigol, M. Bayat, A task-specific phosphonium ionic liquid as an efficient extractant for green desulfurization of liquid fuel: an experimental and computational study, Chem. Eng. J. 295 (2016) 500–508, https://doi.org/10.1016/j.cej.2016.03.072.
[12] F.L. Yu, C.Y. Liu, B. Yuan, P.H. Xie, C.X. Xie, S.T. Yu, Energy-efficient extractive desulfurization of gasoline by polyether-based ionic liquids, Fuel 177 (2016) 39–45, https://doi.org/10.1016/j.fuel.2016.02.063.
[13] J.J. Gao, H. Meng, Y.Z. Lu, H.X. Zhang, C.X. Li, A carbonium pseudo ionic liquid with excellent extractive desulfurization performance, AIChE J. 59 (2013) 948–958, https://doi.org/10.1002/aic.13869.
[14] L.F. Ramirez-Verduzco, F. Murrieta-Guevara, J.L. Garcia-Gutierrez, R. SaintMartin-Castanon, M.D. Martinez-Guerrero, M.D. Montiel-Pacheco, R. Mata-Diaz, Desulfurization of middle distillates by oxidation and extraction process, Pet. Sci. Technol. 22 (2004) 129–139, https://doi.org/10.1081/LFT-120028528.
[15] Y.J. Tian, Y. Yao, Y.H. Zhi, L.J. Yan, S.X. Lut, Combined extraction-oxidation system for oxidative desulfurization (ODS) of a model fuel, Energy Fuels 29 (2015) 618–625, https://doi.org/10.1021/ef502396b.
[16] T. Adzamic, K. Sertic-Bionda, N. Marcec-Rahelic, Modeling of the fcc gasoline desulfurization process by liquid extraction with sulfolane, Pet. Sci. Technol. 28 (2010) 1936–1945, https://doi.org/10.1080/10916460903330056.
[17] A. Bösmann, L. Datsevich, A. Jess, A. Lauter, C. Schmitz, P. Wasserscheid, Deep desulfurization of diesel fuel by extraction with ionic liquids, Chem. Commun. 23 (2001) 2494–2495, https://doi.org/10.1039/B108411A.
[18] R. Martínez-Palou, R. Luque, Applications of ionic liquids in the removal of contaminants from refinery feedstocks: an industrial perspective, Energy Environ. Sci. 7 (2014) https://doi.org/10.1039/C3EE43837F2414–24147.
[19] M.H. Ibrahim, M. Hayyan, M.A. Hashim, A. Hayyan, The role of ionic liquids in desulfurization of fuels: a review, Renew. Sustain. Energy Rev. 76 (2017) 1534–1549, https://doi.org/10.1016/j.rser.2016.11.194.
[20] N. Gathergood, M.T. Garcia, P.J. Scammells, Biodegradable ionic liquids: part I. Concept, preliminary targets and evaluation, Green Chem. 6 (2004) 166–175, https://doi.org/10.1039/B315270G.
[21] A. Romero, A. Santos, J. Tojo, A. Rodriguez, Toxicity and biodegradability of imidazolium ionic liquids, J. Hazard Mater. 151 (2008) 268–273, https://doi.org/10.1016/j.jhazmat.2007.10.079.
[22] A.P. Abbott, D. Boothby, G. Capper, D.L. Davies, R.K. Rasheed, Deep eutectic solvents formed between choline chloride and carboxylic acids: versatile alternatives to ionic liquids, J. Am. Chem. Soc. 126 (2004) 9142–9147, https://doi.org/10.1021/ja048266j.
[23] M. Francisco, A. van den Bruinhorst, M.C. Kroon, Low-transition-temperature mixtures (LTTMs): a new generation of designer solvents, Angew. Chem., Int. Ed. Engl. 52 (2012) 3074–3085, https://doi.org/10.1002/anie.201207548.
[24] C.A. Nkuku, R.J. LeSuer, Electrochemistry in deep eutectic solvents, J. Phys. Chem. B 111 (2007) 13271–13277, https://doi.org/10.1021/jp075794j.
[25] C.M.A. Brett, Deep eutectic solvents and applications in electrochemical sensing, Curr. Opin. Electrochem. 10 (2018) 143–148, https://doi.org/10.1016/j.coelec.2018.05.016.
[26] S.T. Williamson, K. Shahbaz, F.S. Mjalli, I.M. AlNashef, M.M. Farid, Application of deep eutectic solvents as catalysts for the esterification of oleic acid with glycerol, Renew. Eng. 114 (2017) 480–488, https://doi.org/10.1016/j.renene.2017.07.046.
[27] L.I.N. Tomé, V. Baião, W. Silva, C.M.A. Brett, Deep eutectic solvents for the production and application of new materials, Appl. Mater. Today. 10 (2018) 30–50, https://doi.org/10.1016/j.apmt.2017.11.005.
[28] A. Abo-Hamad, M. Hayyan, M.A. AlSaadi, M.A. Hashim, Potential applications of deep eutectic solvents in nanotechnology, Chem. Eng. J. 273 (2015) 551–567, https://doi.org/10.1016/j.cej.2015.03.091.
[29] A. Shishov, A. Bulatov, M. Locatelli, S. Carradori, V. Andruch, Application of deep eutectic solvents in analytical chemistry. A review, Microchem. J. 135 (2017) 33–38, https://doi.org/10.1016/j.microc.2017.07.015.
[30] P. Makoś, A. Przyjazny, G. Boczkaj, Hydrophobic deep eutectic solvents as "green" extraction media for polycyclic aromatic hydrocarbons in aqueous samples, J. Chromatogr. A 1570 (2018) 28–37, https://doi.org/10.1016/j.chroma.2018.07.070.
[31] P. Makoś, A. Fernandes, A. Przyjazny, G. Boczkaj, Sample preparation procedure using extraction and derivatization of carboxylic acids from aqueous samples by means of deep eutectic solvents for gas chromatographic-mass spectrometric analysis, J. Chromatogr. A 1555 (2018) 10–19, https://doi.org/10.1016/j.chroma.2018.04.054.
[32] W.N.A.W. Mokhtar, W.A.W.A. Bakar, R. Ali, A.A.A. Kadir, Deep desulfurization of model diesel by extraction with N,N-dimethylformamide: optimization by Box–Behnken design, J. Taiwan Inst. Chem. Eng. 45 (2014) 1542–1548, https://doi.org/10.1016/j.jtice.2014.03.017.
[33] S.E.E. Warrag, C.J. Peters, M.C. Kroon, Deep eutectic solvents for highly efficient separations in oil and gas industries, Curr. Opin. Green Sustain. Chem. 5 (2017) 55–60, https://doi.org/10.1016/j.cogsc.2017.03.013.
[34] J.M. Silva, R.L. Reis, A. Paiva, A.R.C. Duarte, Design of functional therapeutic deep eutectic solvents based on choline chloride and ascorbic acid, ACS Sustain. Chem. Eng. 6 (2018) 10355–10363, https://doi.org/10.1021/acssuschemeng.8b01687.
[35] J. Li, H. Xiao, X. Tang, M. Zhou, Green carboxylic acid-based deep eutectic solvents as solvents for extractive desulfurization, Energy Fuels 30 (2016) 5411–5418, https://doi.org/10.1021/acs.energyfuels.6b00471.
[36] H. Xu, D. Zhang, F. Wu, X. Wei, J. Zhang, Deep desulfurization of fuels with cobalt chloride-choline chloride/polyethylene glycol metal deep eutectic solvents, Fuel 225 (2018) 104–110, https://doi.org/10.1016/j.fuel.2018.03.159.
[37] C. Li, D. Li, S. Zou, Z. Li, J. Yin, A. Wang, Y. Cui, Z. Yao, Q. Zhao, Extraction desulfurization process of fuels with ammonium-based deep eutectic solvents, Green Chem. 15 (2013) 2793–2799, https://doi.org/10.1039/C3GC41067F.
[38] D. Chandran, M. Khalid, R. Walvekar, N.M. Mubarak, S. Dharaskar, W.Y. Wong, T.C.S.M. Gupta, Deep eutectic solvents for extraction-desulphurization: a review, J. Mol. Liq. 275 (2019) 312–322, https://doi.org/10.1016/j.molliq.2018.11.051.
[39] K.H. Almashjary, M. Khalid, S. Dharaskar, P. Jagadish, R. Walvekar, T.C.S.M. Gupta, Optimisation of extractive desulfurization using Choline Chloride-based deep eutectic solvents, Fuel 234 (2018) 1388–1400, https://doi.org/10.1016/j.fuel.2018.08.005.
[40] F. Lima, J. Gouvenaux, L.C. Branco, A.J.D. Silvestre, I.M. Marrucho, Towards a sulfur clean fuel: deep extraction of thiophene and dibenzothiophene using polyethylene glycol-based deep eutectic solvents, Fuel 234 (2018) 414–421, https://doi.org/10.1016/j.fuel.2018.07.043.
[41] W.S.A. Rahma, F.S. Mjalli, T. Al-Wahaibi, A.A. Al-Hashmi, Polymeric-based deep eutectic solvents for effective extractive desulfurization of liquid fuel at ambient conditions, Chem. Eng. Res. Des. 120 (2017) 271–283, https://doi.org/10.1016/j.cherd.2017.02.025.

MOST WIEDZY Downloaded from mostwiedzy.pl

[42] Z.S. Gano, F.S. Mjalli, T. Al-Wahaibi, Y. Al-Wahaibi, I.M. AlNashef, Extractive desulfurization of liquid fuel with FeCl3-based deep eutectic solvents: experimental design and optimization by central-composite design, Chem. Eng. Process 93 (2015) 10–20, https://doi.org/10.1016/j.cep.2015.04.001.
[43] X. Zhao, G. Zhu, L. Jiao, F. Yu, C. Xie, Formation and extractive desulfurization mechanisms of aromatic acid based deep eutectic solvents: an experimental and theoretical study, Chem. Eur J. 24 (2018) 11021–11032, https://doi.org/10.1002/chem.201803229.
[44] D.V. Wagle, H. Zhao, C.A. Deakyne, G.A. Baker, Quantum chemical evaluation of deep eutectic solvents for the extractive desulfurization of fuel, ACS Sustain. Chem. Eng. 6 (2018) 7525–7531, https://doi.org/10.1021/acssuschemeng.8b00224.
[45] W. Jiang, H. Li, C. Wang, W. Liu, T. Guo, H. Liu, W. Zhu, H. Li, Synthesis of ionic-liquid-based deep eutectic solvents for extractive desulfurization of fuel, Energy Fuels 30 (2016) 8164–8170, https://doi.org/10.1021/acs.energyfuels.6b01976.
[46] D.V. Wagle, G.A. Baker, E. Mamontov, Differential microscopic mobility of components within a deep eutectic solvent, J. Phys. Chem. Lett. 6 (2015) 2924–2928, https://doi.org/10.1021/acs.jpclett.5b01192.
[47] Z. Li, D. Liu, Z. Men, L. Song, Y. Lv, P. Wu, B. Lou, Y. Zhang, N. Shi, Q. Chen, Insight into effective denitrification and desulfurization of liquid fuel with deep eutectic solvents: an innovative evaluation criterion to filtrate extractants using the compatibility index, Green Chem. 20 (2018) 3112–3120, https://doi.org/10.1039/C8GC00828K.
[48] T. Lu, F. Chen, Multiwfn: a multifunctional wavefunction analyzer, J. Comput. Chem. 33 (2012) 580–592, https://doi.org/10.1002/jcc.22885.
[49] T. Lu, F. Chen, Quantitative analysis of molecular surface based on improved Marching Tetrahedra algorithm, J. Mol. Graph. Model. 38 (2012) 314–323, https://doi.org/10.1016/j.jmgm.2012.07.004.
[50] E.R. Johnson, S. Keinan, P. Mori-Sanchez, J. Contreras-Garcıa, A.J. Cohen, W. Yang, Revealing noncovalent interactions, J. Am. Chem. Soc. 132 (2010) 6498–6506, https://doi.org/10.1021/ja100936w.
[51] H.R. Lozano, F. Martínez, Thermodynamics of partitioning and solvation of ketoprofen in some organic solvent/buffer and liposome systems, Braz. J. Pharm. Sci. 42 (2006) 601–613, https://doi.org/10.1590/S1516-93322006000400016.
[52] M. Jafari, S.L. Ebrahimi, M.R. Khosravi-Nikou, Ultrasound-assisted oxidative desulfurization and denitrogenation of liquid hydrocarbon fuels: a critical review, Ultrason. Sonochem. 40 (2018) 955–968, https://doi.org/10.1016/j.ultsonch.2017.09.002.
[53] C. Li, J. Zhang, Z. Li, J. Yin, Y. Cui, Y. Liua, G. Yang, Extraction desulfurization of fuels with 'metal ions' based deep eutectic solvents (MDESs), Green Chem. 18 (2016) 3789–3795, https://doi.org/10.1039/C6GC00366D.
[54] US Patent US2050600A, Production and Purification of Diethyl Ether, 1933.
[55] US Patent US3847756A, Recovery of Diethyl Ether from an Olefin Hydration Product Stream by Extractive Distillation with Water, 1972.
[56] J. Yanowitz, M.A. Ratcliff, R.L. McCormick, J.D. Taylor, M.J. Murphy, Compendium of Experimental Cetane Numbers, National Renewable Energy Laboratory, 2017. https://www.nrel.gov/docs/fy17osti/67585.pdf, Accessed date: 14 January 2019.
[57] G. Jeffrey, An Introduction to Hydrogen Bonding, Oxford University Press, 1997.
[58] H.S. Biswal, S. Chakraborty, S. Wategaonkar, Experimental evidence of O–H–S hydrogen bonding in supersonic jet, J. Chem. Phys. 129 (2008) 184311, https://doi.org/10.1063/1.3012569.
[59] H.S. Biswal, S. Wategaonkar, Sulfur, not too far behind O, N, and C: SH···π hydrogen bond, J. Phys. Chem. A 113 (2009) 12774–12782, https://doi.org/10.1021/jp907747w.
[60] H.S. Biswal, P.R. Shirhatti, S. Wategaonkar, O–H···O versus O–H···S hydrogen bonding I: experimental and computational studies on the p-cresol···H2O and p-cresol···H2S complexes, J. Phys. Chem. A 113 (2009) 5633–5643, https://doi.org/10.1021/jp9009355.
[61] S. Bhattacharyya, A. Bhattacherjee, P.R. Shirhatti, S. Wategaonkar, OH···S hydrogen bonds conform to the acid–base formalism, J. Phys. Chem. A 117 (2013) 8238–8250, https://doi.org/10.1021/jp405414h.
[62] S. Kumar, A. Das, Effect of acceptor heteroatoms on -hydrogen bonding interactions: a study of indolethiophene heterodimer in a supersonic jet, J. Chem. Phys. 137 (2012), 094309. https://doi.org/10.1063/1.4748818.
[63] J.A. Platts, S.T. Howard, B.R.F. Bracke, Directionality of hydrogen bonds to sulfur and oxygen, J. Am. Chem. Soc. 118 (1996) 2726–2733, https://doi.org/10.1021/ja952871s.
[64] J. Zhu, K. Yu, Y. Zhu, R. Zhu, F. Ye, N. Song, Y. Xu, Physicochemical properties of deep eutectic solvents formed by choline chloride and phenolic compounds at T = (293.15 to 333.15) K: the influence of electronic effect of substitution group, J. Mol. Liq. 232 (2017) 182–187, https://doi.org/10.1016/j.molliq.2017.02.071.
[65] W. Jiang, L. Dong, W. Liu, T. Guo, H. Li, S. Yin, W. Zhu, H. Li, Biodegradable choline-like deep eutectic solvents for extractive desulfurization of fuel, Chem. Eng. Process 115 (2017) 34–38, https://doi.org/10.1016/j.cep.2017.02.004.

MOST WIEDZY Downloaded from mostwiedzy.pl